HHS Public Access

Author manuscript

Mucosal Immunol. Author manuscript; available in PMC 2019 April 12.

Published in final edited form as:

Mucosal Immunol. 2019 January ; 12(1): 212–222. doi:10.1038/s41385-018-0082-8.

Characterization of CD28^{null} T cells in Idiopathic Pulmonary Fibrosis

David M Habiel[1,*], **Milena S Espindola**[1], **Chris Kitson**[2], **Anthony V Azzara**[2], **Ana Lucia Coelho**[1], **Barry Stripp**[1], and **Cory M Hogaboam**[1,*]

[1]Women's Guild Lung Institute, Department of Medicine, Cedars-Sinai Medical Center, Los Angeles, CA 90048.

[2]Bristol-Myers Squibb, Fibrosis Discovery Biology, Pennington, NJ 08534

Abstract

Idiopathic pulmonary fibrosis (IPF) is a fibrotic lung disease, with unknown etiopathogenesis and suboptimal therapeutic options. Previous reports have shown that increased T cell numbers and CD28^{null} phenotype is predictive of prognosis in IPF, suggesting that these cells might have a role in this disease. Flow cytometric analysis of explanted lung cellular suspensions showed a significant increase in CD8^{+} CD28^{null} T cells in IPF relative to normal lung explants. Transcriptomic analysis of CD3^{+} T cells isolated from IPF lungs explants revealed a loss of CD28 transcript expression and elevation of proinflammatory cytokine expression in IPF relative to normal T cells. IPF lung explant derived T cells (enriched with CD28^{null} T cells), but not normal donor lung CD28^{+} T cells induced dexamethasone resistant lung remodeling in humanized NSG mice. Finally, CD28^{null} T cells expressed similar CTLA4 and significantly higher levels of PD-1 proteins relative to CD28^{+} T cells and blockade of either proteins in humanized NSG mice, using anti-CTLA4, or anti-PD1, mAb treatment accelerated lung fibrosis. Together, these results demonstrate that IPF CD28^{null} T cells may promote lung fibrosis but the immune checkpoint proteins, CTLA-4 and PD-1, appears to limit this effect.

Introduction:

Despite the advent of approved pharmacological interventions, IPF remains one the most challenging interstitial lung diseases to manage clinically[1]. The fibrotic triggers in IPF are unknown but it is speculated that persistent lung injury leads to alveolar epithelial cell injury and death, and subsequent aberrant repair mechanism(s) ablates the alveolus[2]. Recently, two new therapeutics have been FDA approved for the treatment of IPF patients, Ofev™ and

*Correspondence: David.Habiel@cshs.org, (310) 967-3817, Cedars-Sinai Medical Center, 127 S San Vicente Blvd., AHSP A9404, Los Angeles, CA 90048, Cory.Hogaboam@cshs.org, (424) 315-2862, Cedars-Sinai Medical Center, 127 S San Vicente Blvd., AHSP A9315, Los Angeles, CA 90048.

Author Contributions:

DMH conceived experiments, performed experiments, analyzed results and wrote and edited the manuscript. MSE and ALC performed experiments. CK and AVA conceived experiments, provided reagents and edited the manuscript. BS helped with patient and normal donor tissue procurement. CMH conceived experiments, wrote and edited manuscript.

The authors have declared that no conflict of interest exists.

Esbriet™, both of which were effective at slowing down disease progression. Unfortunately, neither therapeutic were effective at halting disease progression. Thus, many studies have focused on understanding mechanisms leading to the progressive decline of lung function in IPF patients to ultimately develop more effective second-generation therapeutics.

Experimental evidence and histological analysis indicate that there are multiple mechanisms, involving various cellular compartments that culminates into the progressive remodeling of the lung. Several studies have reported evidence for the injury and loss of the reparative Type II alveolar epithelial cells, leading to aberrant stromal activation and disrepair in IPF lungs. The origin of epithelial injury in IPF is controversial; however, studies have suggested various sources including pathogens[3], ER stress[4] and immune activation[5–9]. Indeed, experimental evidence and histological analysis indicate that there are innate and adaptive immune cells, particularly lymphocytes[10], which might contribute to alveolar destruction and progressive remodeling of the lung. The accumulation of $CD3^+$ T cells and $CD20^+$ B cells in lymphocyte aggregates is well documented in the IPF lungs[10] and a high prevalence of monoclonality and oligoclonality[9,11,12], suggesting that lymphocytes may contribute to the pathological remodeling observed in the lungs of these patients. However, given the failure of immunomodulatory therapeutics in IPF[13], the role of immune cells and immune cell activation in this disease remains controversial.

The phenotype of T cells in IPF has been poorly characterized. Few studies have reported that peripheral blood IPF T cells exhibit a surface and/or gene expression signature characterized by a loss of one or more costimulatory molecules, including CD28 and ICOS receptors and a negative correlation between progression-free survival and the abundance of $CD28^{null}$ T cells in IPF patients[8, 14] $CD28^{null}$ T cells are antigen experienced memory T cells that are observed in multiple pathological conditions, including COPD[15–17], kidney disease[18], rheumatoid arthritis[19] and myositis[20, 21]. These cells have been observed to possess shortened telomeres[18, 22], markers of senescence[18, 23–25] and to abundantly secrete IFNγ, TNFα, perforin and granzymes[19, 23]. Further, these cells may be resistant to corticosteroid treatment[15–17, 20, 21, 26] and several studies have correlated their abundance with cytomegalovirus infection[18, 27, 28]. Given that these cells are often observed in chronic disease settings, where tissue fibrosis is often an outcome, further investigation of profibrotic and injurious mechanisms elaborated by $CD28^{null}$ T cells in IPF is warranted.

In this report, a detailed characterization of the phenotype and function of IPF lung-derived T cells is provided. There was a significant increase in the number of $CD28^{null}$ cytotoxic $CD8^+$ T cells in IPF relative to normal explanted lung cellular suspensions. Transcriptomic analysis confirmed the overall loss of CD28 expression in IPF lung relative to normal donor blood derived T cells, where cells showing the lowest CD28 expression highly expressed transcripts involved in lysosomal and proinflammatory functions. $CD28^{null}$ enriched IPF, but not $CD28^+$ enriched normal, T cells induced more consistent, dexamethasone resistant, lung remodeling in humanized NSG mice. Flow cytometric analysis suggested that $CD28^{null}$ T cells express similar levels of CTLA4 and significantly higher PD-1 proteins. Further, there was a significant increase in the percentage of PD-L1-expressing $EpCAM^+$ and $CD45^-$ $EPCAM^-$ cells in IPF relative to normal lungs. Finally, anti-CTLA4 or anti-PDI mAb, treatment of humanized NSG mice exacerbated pulmonary fibrosis, with the former

treatment correlating with an expansion of IPF T cells in these mice. Collectively, these results demonstrate that CD28^{null} T cells present in IPF lung have the potential to drive fibrotic mechanisms, but immune checkpoint protein expression might impede this process.

Results:

Abundance of CD3^{+} CD8^{+} CD28^{null} T cells in explanted IPF lung tissues.

Several studies have observed a correlation between the number of CD28^{null} helper CD4^{+} T cells and prognosis[8, 14] However, these studies examined T cells from the peripheral blood of IPF patients. Thus, studies examining the relative abundance of CD28^{+} versus CD28^{null} T cells from normal and IPF explanted lung tissues were performed. Flow cytometric analysis of immune cells released after mechanical dissociation of explanted normal and IPF lung tissues showed similar levels of CD45^{+} immune (Figure 1A–B) and CD45^{+} CD3^{+} T cells (Figure 1C–D) recovered from both lung explants. There was a significant increase in the percentage of CD4^{+} helper (Figure 1E–F) and CD8$_{+}$ cytotoxic (Figure 1E & 1G) T cells in IPF relative to normal lungs. Further, there was similar levels of CD28^{+} and CD28^{null} CD4^{+} helper T cells (Figure 1H–J), CD28^{+} CD8^{+} cytotoxic T cells (Figure 1K–L) and a significant increase in the percentage of CD28^{null} CD8^{+} cytotoxic T cells (Figure 1K & 1M) in IPF relative to normal lungs. These results suggest that there is a significant increase in the number of CD28^{null} cytotoxic T cells in IPF lungs.

Flow cytometric analysis showed that CD3^{+} CD4^{+} CD28^{+} T cells from normal and IPF explanted lung tissues predominately expressed CD45RO, with fewer cells expressing CD45RA (Figure S1A–B, left panels; quantified in Figure S1E, left panels). Further, there was a significant reduction in the percentage of CD45RO^{+} CD4^{+} helper T cells in IPF relative to normal lung explant tissues (Figure S1E, bottom left panel). Consistent with published reports showing that CD4^{+} CD28^{null} T cells expressed markers of highly antigen mature, memory T cells (including CD45RO[29, 30]), CD28^{null} helper CD4^{+} T cells predominately expressed CD45RO but not CD45RA in both normal and IPF lung tissues (Figure S1A–B, right panels; quantified in Figure S1E, right panels). Further, most CD28^{+} CD8^{+} cytotoxic T cells in normal and IPF explanted lung tissues expressed CD45RO, with few cells expressing CD45RA (Figure S1C–D, left panels; quantified in Figure S1F, left panels). Unexpectedly, there were populations of CD28^{null} CD8^{+} cytotoxic T cells expressing CD45RA or CD45RO in both normal and IPF explanted lung tissues (Figure S1 C–D, right panels; quantified in Figure S1F, right panel). These results suggest that while CD4^{+} CD28^{null} T cells predominately express the memory T cell associated CD45RO antigen, CD8^{+} CD28^{null} cytotoxic T cells were observed to express CD45RA or CD45RO in lung tissues.

Enrichment of T cell activation and proinflammatory pathways in IPF lung T cells.

Various studies have reported that T cells from IPF patients are phenotypically and functionally distinct from T cells derived from normal donors[8, 14] Specifically, IPF T cells exhibit monoclonal and oligoclonal properties[9, 11, 12], and react to autoantigens[6]. In the present study, RNAseq data analysis of lung explant derived IPF T cells and normal peripheral T cells revealed that there were approximate 1850 transcripts significantly

differentially expressed in IPF compared normal T cells (Figure 2A). According to KEGG pathway analysis, T cell activation pathways (including Viral Myocarditis, Graft-versus-host disease, allograft rejection, type I diabetes mellitus, autoimmune thyroid disease, rheumatoid arthritis, influenza A and others) were enriched in IPF relative to normal T cells (Table S1). Ingenuity upstream analysis predicted the activation of various pro-inflammatory mediators, (including *TNF, IL1-β, IL6* and *IFN-γ)*, microbial sensors (including *TLR2, TLR3, TLR4, TLR7* and *TLR9)* and profibrotic mediators (including *PDGF-BB, TGF-β1, IL18*, and *IL13)* in IPF relative to normal T cells (Table S2). Indeed, there was an enrichment of various transcripts previously shown to be abundantly expressed and/or to play a role in pulmonary remodeling in IPF relative to normal T cells (Figure 1B). Further, there was no evidence for Th2 or Th17 skewing in these cells based upon the lack of transcripts encoding for *IL17, IL4*, and *IL13* (data not shown) and no evidence for consistent predominance of *FOXP3, TGFb, IFNg, GZM* expressing T cells in IPF relative to normal T cells (Figure 2C). These results suggest that IPF T cells are distinct from normal T cells via their expression of transcripts involved in T cell activation, inflammation, microbial sensing and fibrosis.

To better characterize the transcriptome of $CD28^{null}$ T cells in IPF, transcriptomic datasets were mined for CD28 expression. This analysis was performed on FACS sorted T cells from three IPF patients (i.e. IPF1, IPF2 and IPF3) and three magnetically sorted peripheral blood $CD4^+$ helper T cells (i.e. Normal 1, Normal 2 and Normal 3). There was an overall loss of CD28 transcript in IPF T cells, with IPF1 showing an almost complete loss of CD28 Transcript (Figures 2C & S2). CD28-low expressing IPF1 T cells expressed a very distinct transcriptome and clustered separately than IPF2 & IPF 3 T cells (Figure 2A). To determine the pathways enriched in $CD28^{null}$ IPF T cells, Ingenuity and KEGG pathway analysis was performed comparing IPF1 (low CD28) to IPF2 (high CD28) T cells. KEGG pathway analysis showed an enrichment of lysosomal and phagosomal transcripts (especially transcripts encoding for lysosomal and phagosomal proteases) in IPF1 relative to IPF2 T cells (Table S3 & Figure 1D). Ingenuity upstream analysis predicted the activation of proinflammatory and profibrotic mediators (IFNG, IL5, TGFB1, TNF, NFkB, IL4, IL1B, IL6, STAT4, PDGFBB) in IPF1 relative to IPF2 T cells (Table S4). Finally, Ingenuity comparison analysis of IPF1 vs IPF2 and $CD28^{null}$ vs $CD28^+$ $CD4^+$ T cells (GSE78942[31]) showed similar upstream regulators (including IL1ß, TGFß1, TNF, IFNg, IL6 & IL5; Table S5) and ingenuity causal networks (Table S6) predicted to be active in IPF1 and $CD28^{null}$ T cells. These results suggest that IPF1 T cells are highly enriched for $CD28^{null}$ T cells and that these cells express many pro-inflammatory and pro-fibrotic mediators.

Activated $CD28^{null}$ T cells have similar cytotoxicity to activated $CD28^+$ T cells.

Several reports have suggested that $CD28^{null}$ T cells have shortened telomeres[18, 22], express markers of senescence and may have altered effector functions[18, 23–25]. Indeed, there was an enrichment in senescence-associated markers in IPF (especially in IPF1 T cells) relative to normal T cells (Figure S3A). Further, consistent with the previously described reports of alternative co-stimulatory protein and pathway expression in $CD28^{null}$ T cells[23, 32], IPF1 T cells showed a distinct expression pattern of co-stimulatory kinases and receptors (Including SRC, HRAS, HCK, SYK, CD40 and CD31; Figure S3B). To functionally assess the cytotoxicity of $CD28^+$ versus $CD28^{null}$ T cells in IPF, $CD28^+$ and $CD28^{null}$ T cells were

magnetically enriched or FACS sorted and then co-cultured with RFP expressing A549 cells in the presence of activating CD3/CD28 chimeric antibodies (STEMCELL Technologies). The proliferation of A549 epithelial cells cultured alone or co-cultured with sorted T cells was monitored using an Essen Bioscience live cell imager over a span of 3–5 days. Over the time points analyzed, A549 epithelial cells rapidly proliferated to confluency (Figure 3A), however, activated $CD28^{+}$ (Figure 3B), and to a lesser extent, $CD28^{null}$ (Figure 3C), T cells induced a marked reduction of overall A549 cell numbers over the duration of the experiments (Figure 3D–F). In these studies, most of the patients tested required activating CD3/CD28 antibodies for T cell responses on the co-cultured A549 cells (Figure S4A); however, $CD28^{null}$ T cells from a subset of IPF patients strongly reacted to A549 cells in the absence of activating antibodies (Figure S4B). These results suggest that $CD28^{+}$ and $CD28^{null}$ T cells may possess similar cytotoxic potential.

Isolated IPF1 T cells induced dexamethasone resistant pulmonary fibrosis in humanized NSG mice.

Due to yield limitations in number of T cells required for *in vivo* analysis, functional analysis of $CD28^{null}$ T cells was performed using cells from IPF1 and compared to those from a normal donor (whose cells abundantly express CD28). Normal and IPF1 T cells were magnetically sorted and intravenously injected into NODCg-Prkdc<SCID> IL2rg<Tm1wil>Szi (NSG) mice. Sixty-five days after the injection of 1 × 104 T cells from normal or IPF lung explants, Masson's trichrome staining revealed more consistent interstitial fibrosis in the lungs of NSG mice challenged with IPF T cells (Figure 4D) but not in lungs of mice that received normal T cells (Figure 4B), which were similar to naïve NSG mouse lungs (Figure 4A). There was greater picrosirius red staining in the subpleural and interstitial lung regions in NSG mice that received IPF (Figure 4E) relative to normal (Figure 4C) T cells. Human $CD45^{+}$ cells were detected in the lungs and the spleen of the humanized NSG mice (Figure 4F–G, **left panels, respectively)**, and these cells expressed low levels of surface CD3ε protein (Figure 4F–G, **right panels, respectively)**. Finally, there was a significant increase in hydroxyproline in the lungs of NSG mice that receive IPF relative to normal T cells (Figure 4H).

To determine potential mechanisms through which IPF T cells promoted fibrosis in NSG mice, protein analysis of the bronchoalveolar lavage (BAL) fluid was performed for various markers of lung injury and inflammation. Compared with BAL from naïve NSG mice, there was modest, but progressive, decrease in the levels of surfactant protein C in the lungs of NSG mice that normal and IPF T cells (Figure 4I). This decline did not appear to be the result of enhanced inflammatory responses because murine-IL12-p70, TNFα and IFNγ were modestly reduced or unchanged in the humanized NSG groups compared with the naïve NSG group (Figure 4J). Thus, these results demonstrate that IPF T cells appear to be targeting mouse type 2 epithelial cells rather than evoking an inflammatory response in the lungs of humanized NSG.

Given the failure of immunomodulatory therapeutics in IPF[13], the role of immune cells and immune cell activation in this disease remains controversial. However, several reports have suggested that $CD28^{null}$ T cells are resistant to Immunosuppressants clinically[15–17, 26].

Thus, to assess the sensitivity of IPF CD28^{null} T cells to corticosteroids, 2 × 10^5 IPF1 T cells were intravenously administered into NSG mice two hours after intraperitoneal treatment with dexamethasone (10 mg/kg). Mice were then treated with the immunosuppressant twice a week for a total of 5 weeks. As a control, untreated, IPF1 T cell challenged and naïve, non-humanized, mice were utilized. After a total of 5 weeks, mice were sacrificed, and their lungs were collected for histological and biochemical analysis. Relative to naïve lungs (Figure 5A), untreated IPF1 T cells induced focal areas of interstitial consolidation and blue trichrome staining (Figure 5B), which was more consistently observed after dexamethasone treatment (Figure 5C). Biochemical analysis of hydroxyproline concentration in NSG lung tissues suggested that IPF1 T cells induced a trending (albeit non-consistent) increase in hydroxyproline content in the lungs; however, dexamethasone treatment of IPF1 T cell challenged mice induced a consistent and significant elevation in hydroxyproline content in the lungs relative to naïve NSG mice (Figure 5D). Further, mining of transcriptomic datasets for transcript expression of genes that has been previously shown to play a role in the resistance of CD28null T cell to immunosuppressive therapy[15–17, 33] showed that IPF 1 T cells had markedly reduced *NR3C1* and HDAC2 transcript expression, and increased HSP90 transcript expression relative to other IPF and normal T cells (Figure S5). These results suggest that CD28^{null}-rich IPF1 T cells may be resistant to the immunosuppressant, dexamethasone.

CD28^{null} T cells express similar levels of CTLA4 and significantly higher levels of PD-1 protein relative to CD28^{+} cells.

Consistent with previous reports[8, 14], transcriptomic analysis showed that there was an overall loss of co-stimulatory proteins in the CD28^{null}-rich IPF1 T cells relative to IPF2, IPF3 and normal T cells (Figure S3B). This phenotype is consistent with T cell phenotypes that have been previously described in aged and immune checkpoint-regulated T cells[25, 34, 35]. Further, there was no conclusive or consistent evidence for T cell activation and/or T cell mediated autoimmunity in the IPF patients examined elsewhere or herein. Consequently, we hypothesized that host-mediated immunomodulatory mechanisms such as immune checkpoint pathways may modulate the activity of CD28^{null} T cells. Flow cytometric analysis of normal and IPF T cells showed that CD28^{+} and CD28^{null} CD4^{+} helper T cells express similar cell surface levels of CTLA4 (Figure 6A) and PD-1 (Figure 6B) proteins. However, flow cytometric analysis of CD8^{+} cytotoxic T cells showed that CD28^{null} cells express similar levels of CTLA4 (Figure 6C) and significantly higher levels of PD-1 (Figure 6D) proteins relative to CD28^{+} cytotoxic T cells. Similar analysis for PD-L1 indicated that this ligand was significantly reduced on CD45^{+} immune cells in IPF compared with normal lungs (Figure 6E–F). However, there was a significant elevation in the expression of PD-L1 in IPF CD45^{-} EpCAM^{+} cells (Figure 6G–H), and CD45^{-} EpCAM^{-} cells (Figure 6I–J) relative to their normal counterparts. Collectively, these results suggested that IPF lungs have significantly higher levels of CD8^{+} cytotoxic CD28^{null} T cells, which express significantly higher levels of the immune checkpoint protein PD-1. Further, there was a significant increase in the percentage of structural cells in IPF lungs expressing PD-L1 protein relative to their normal counterparts.

Immune checkpoint inhibitors exacerbated pulmonary fibrosis and the expansion of human T cells in humanized NSG mice.

To assess the role of immune checkpoint proteins in T cell mediated lung remodeling in humanized NSG mice, a modification of the humanized NSG model was introduced, where cells expressing immune checkpoint ligands and T cells were administered into NSG mice, as previously described36. In this model, lung remodeling is observed starting at 35 and more consistently after 63 days after the intravenous injection of immune and non-immune IPF cells into NSG mice (including $EpCAM^+$ epithelial cells, PDGFR-$alpha^+$ and PDGFR-$beta^+$ stromal cells, $SSEA4^+$ progenitor cells, $CD31^+$ cells, $CD3^+$ T cells, $CD19^+$ B cells, $CD335^+$ cells and $CD45^+$ $CD138^+$ plasma cells, as previously described[36]). Flow cytometric analysis of humanized NSG lung tissues, 63-days after IPF explant cell administration revealed that human $CD3^+$ cells were present in the lungs (Figure S6A–C **and quantified in** S6D) and spleens (Figure S6E–G **and quantified in** S6H) of the injected NSG mice. These studies demonstrate that human T cells engraft in NSG mice after the intravenous introduction of immune and non-immune IPF cells and this coincides with lung fibrosis in humanized NSG mice.

We next examined the effects of checkpoint targeting mAbs on the lung fibrosis elicited by the intravenous introduction of IPF cells into NSG mice. Compared with naïve NSG mice (Figure 7A), humanized NSG mice that received anti-CTLA-4 (Figure 7D) or anti-PD-1 (Figure 7F) mAb exhibited histologic evidence of mild interstitial consolidation compared with saline-treated (Figure 7B) and the IgG-treated (Figure 7C & 7E) NSG mouse groups. Further, there was a significant elevation in hydroxyproline in the anti-CTLA-4 and anti-PD-1 mAb-treated groups compared with the respective IgG control NSG group (Figure 7G). Anti-CTLA4 mAb treatment increased the numbers of human-$CD3_+$ cells (Figure 7H) and murine $F4/80^+$ $CD11c^-$ macrophages (Figure S7B) compared with the appropriate IgG control group. Finally, there were no significant changes in the number of mouse myeloid cells ($F4/80^+$ $CD11c^+$, $F4/80^-$ $CD11c^+$ and $F4/80^-$ $Ly6G^+$ cells) in the lungs of any of the NSG mouse groups (Figure S7A & S7C–D). Thus, these results demonstrate that targeting PD-1 or CTLA4 accelerated fibrosis in a translational NSG model of pulmonary fibrosis.

Discussion:

While the precise role of the immune system on the progression of IPF remains controversial, recent evidence suggest that immune pathways may be aberrantly activated in this disease[5, 7] These findings provided the impetus to further characterize various immune cell populations in IPF lungs and to determine the roles of these cells in disease initiation and progression. The data present herein indicated that there is an abundance of cytotoxic $CD8^+$, but not helper $CD4^+$, $CD28^{null}$ T cells in explanted IPF lungs relative to normal donor lungs. These finding are inconsistent with one study showing the abundance of $CD4^+$ $CD28^-$ T cells in IPF patients' blood[8], potentially due to differences between the circulating and lung-associated T cell populations, as previously suggested[37], or heterogeneity within different cohorts of IPF patients. There was a significant difference in the age of the IPF patients and normal lung donors (Mean66.8 versus 52.8, respectively; p=0.0137), thus, it is possible that differences in the abundance of $CD28^{null}$ T cells observed in our studies may

be in-part due to the age differences IPF and normal donors. Future studies are warranted to confirm our findings in other cohorts of IPF patients.

In vivo studies suggested that IPF CD28^{null} T cells may promote dexamethasone-resistant lung fibrosis, when administered alone (i.e. in the absence of other immune and non-immune cells). These studies were performed with T cells from an IPF patient (IPF1) showing relatively low levels of CD28 transcript (Figure S2), which induced lung remodeling as early as day 35 but more consistently after 63–65 days. In addition to showing reduced CD28 transcript expression, cells from IPF1 showed reduced expression of other co-stimulatory proteins, including ICOS, CD137 and BTLA, suggesting that CD28 is not uniquely lost on these cells and that there may be a global loss of co-stimulatory proteins on these cells. Interestingly, dexamethasone seemed to accelerate IPF1 T cell induced lung fibrosis in NSG mice, as evident by histological analysis and consistent elevation of hydroxyproline concentration after 35 days of T cell administration and dexamethasone treatment. Mechanisms leading to dexamethasone resistance in IPF CD28^{null} T cells remain elusive; however, our transcriptomic data suggests that downregulation of glucocorticoid receptor and HDAC2 transcript expression may play a role, similar to what has been reported in CD28^{null} T cells in COPD[38, 39]. However, HSP90, a chaperone that has been previously observed to promote corticosteroid binding to glucocorticoid receptor[17], was elevated in IPF1 T cells, suggesting that this protein may partially rescue any potential deficiencies to corticosteroid responses mediated by reduced glucocorticoid receptor expression. Future work is warranted to better understand the extent of immunosuppressive resistance of IPF CD28^{null} T cells and to identify therapeutic mechanisms that may directly target these cells or sensitize them to immunosuppressive therapy.

Due to limitations in the number of cells recovered from explanted lung tissues, studies examining differences between CD28^{+} versus CD28^{null} and CD4^{+} CD28^{null} versus CD8^{+} CD28^{null} T cells from the same explanted lung tissues were not possible. This limitation can be potentially overcome by the use of peripheral blood T cells from these patients; however, differences in circulating versus lung associated T cell populations, as recently suggested[37], may lead to differing responses in NSG mice. While CD28^{null} T cells are rarely detected in mice[40], one study have shown that CD8^{+} CD28^{null} T cells may expand in the pulmonary airways of mice in response to cigarette smoke[41]. Thus, future studies utilizing mouse models of fibrosis may help further characterize the role(s) of these cells in lung injury, remodeling and repair.

Loss of CD28 on T cells is a feature of antigen experienced, highly differentiated and aged T cells[25, 35, 42], a finding that is consistent with the limited IPF T cell receptor repertoire observed by others[6, 9, 11, 12], Given that IPF CD28^{null} T cells were previously reported to be stimulated with anti-CD3 antibodies alone (i.e. in the absence of co-stimulatory signal activation)(1), and the lack of co-stimulation of CD28^{+} T cells may lead to their anergy (2), we have decided to stimulate both CD28^{+} and CD28^{null} T cell groups with a tetrameric complex of anti-CD3 and -CD28 antibodies (STEMCELL technologies). This approach ensured that both groups are efficiently activated, thus allowing for adequate comparison of their cytotoxic potential. Despite the loss of CD28, CD28^{null} T cells showed similar *in vitro* cytotoxic potential relative to their CD28^{+} counterparts. Transcriptomic analysis of CD28-

transcript-low IPF1 T cells revealed an abundance of T cell activation and autoimmune pathways, inflammasome and pro-inflammatory cytokine expression and similar upstream regulator activation to previously characterized $CD28^{null}$ T cells[31]. Indeed, similar expansion and/or responses of $CD28^{null}$ T cells have been previously reported in inflammatory disorders, including atherosclerosis, chronic viral infection and autoimmunity[42] and IPF[8].

Using a humanized NSG model that is initiated via the intravenous introduction of $CD28^{null}$-enriched T cells purified from IPF1 lung explants, adoptively transferred T cells induced lung remodeling that was most consistent after 63–65 days of cell injection into NSG mice. One potential mechanism leading to this observed remodeling by IPF T cells is the loss of BAL surfactant protein C in IPF1 humanized NSG mice. While the levels of surfactant protein C were not significantly altered, relative to naïve mice, the levels of this protein were consistently reduced in the BAL of IPF1 T cell humanized mice, suggesting a loss of alveolar type II epithelial cells or the modulation of surfactant protein C expression by these cells. Indeed, several studies have shown that dysfunction or injury of alveolar type II epithelial cells promotes interstitial lung remodeling in mice[43] and that surfactant homeostasis is required to lower surface tension during normal respiration, thus maintaining normal alveolar structures and decreasing susceptibility to injury[44]. Further, in our *in vitro* studies, a subset of IPF patients possessed T cells that were cytotoxic to A549 epithelial cells in the absence of T cell receptor activating antibodies, suggesting that these cells may be reactive A549 cells, a cell like that expresses many proteins that are specifically expressed by Alveolar type II epithelial cells. Thus, our results suggest that $CD28^{null}$ T cells may promote lung remodeling by targeting alveolar type II epithelial cells or by modulating surfactant protein C production by these cells.

With the recent success of immune checkpoint inhibitors in treating various solid tumors, immune checkpoint pathways have been an active area of investigation[45, 46]. These pathways have been shown to regulate the activation of acquired immune cells, especially T cells via receptor-ligand signaling and soluble mediators[45–47]. The most studied (and clinically targeted) immune checkpoint proteins include PD-1 (and its ligands, PD-L1 and PD-L2) and CTLA-4, which are often elevated in chronic infection and cancer[45–47]. Transcriptomic analysis of IPF1 T cells suggested that these cells abundantly expressed *PDCD1* and *CTLA4* transcripts. Flow cytometric analysis on $CD28^{null}$ cytotoxic T cells showed higher levels of PD-1 receptor on these cells relative to $CD28^{+}$ cytotoxic T cells. Further, there was an abundance of PD-L1 expression by structural cells in IPF relative to normal lung samples. When anti-CTLA-4 mAb or anti-PD-1 mAb were used in humanized NSG mice, both mAbs significantly increased lung fibrosis compared with the appropriate IgG-treated NSG group. In addition, anti-CTLA-4 mAb treatment was associated with increased human T cell engraftment and/or proliferation compared with the IgG-treated NSG group. In these studies, we observed no significant differences in BAL surfactant protein C (not shown), in neutrophils or inflammatory mediators in humanized NSG mice compared with naïve NSG mice. There was no evidence of cellular infiltration or injury in the liver or kidney of humanized NSG mice suggesting that the fibrotic response induced by IPF cells in the lungs of NSG mice was not due to graft-versus-host disease. These results suggest that immune checkpoint mediated lung remodeling may be driven through different

mechanisms that what was observed in IPF1 T cells humanized NSG mice, potentially due to the differences in human cell populations present in these two humanized NSG models (i.e. T cells alone or immune and structural cells). It is possible that proinflammatory cytokines and chemokines may be released by T cells in response to checkpoint inhibition, which may act on other human cells to promote lung remodeling. Collectively, our results demonstrate that profibrotic CD28null T cells are elevated in IPF lung tissues that CTLA-4 and PD-1 might protect against fibrosis in IPF via its modulation of T cells poised to initiate profibrotic mechanisms.

Materials and Methods:

Study approval:

Institutional Review Board approval for the studies outlined herein was obtained at Cedars-Sinai Medical Center. Informed consent was obtained from all patients prior to inclusion in the studies described herein. Cedars-Sinai Medical Center Department of Comparative Medicine approved all mouse studies described herein. All studies were performed in accordance with the relevant State and Federal guidelines and regulations.

Isolation of IPF explant cells and T cell sorting for *in vivo* studies:

Normal and IPF lung explants were acquired from consented donors. The demographics of the normal donor lung tissues and IPF patients utilized in RNAseq, flow cytometric analysis and NSG studies are provided in Table S7. The mean age of the normal donors and IPF patients were 52.8 and 66.8, respectively ($p=0.0137$ via Mann Whitney two-tailed non-parametric T test). Fresh explant cells were isolated are previously described[36]. For *in vivo* experiments, cells were rapidly thawed, washed in serum free medium and intravenously injected into NSG mice as described below. To isolate T cells for NSG studies, T cells were magnetically sorted from freshly thawed bio-banked explant cells using anti-human CD3 microbeads (Miltenyi Biotech, 130-050-101). Sorted cells were then cultured on plastic dishes for 2 hours to deplete any contaminating antigen presenting cells, after which 100,000 cells were intravenously injected into NSG mice.

In vitro assessment of T cell cytotoxicity.

RFP-expressing A549 epithelial cells were plated onto a 96 well plate at a concentration of 2500 cells/well and incubated overnight at 37 °C and 10% CO_2. The next morning, bio-banked IPF lung explant suspensions were thawed out and $CD3^+$ T cells were magnetically enriched using releasable magnetic beads (STEMCELL Technologies). $CD3^+$ cells were then stained with anti-CD28-APC (Biolegend) and $CD28^+$ cells were enriched using anti-APC magnetic beads (STEMCELL Technologies). After enrichment, A549 cells were washed and 6×10^4 non-bound cells ($CD28^{null}$) and CD28 enriched ($CD28^+$) cells were added onto the A549 epithelial cells in RPMI + 15% FBS (Atlanta Biological), 100 IU penicillin and 100 μg/ml streptomycin (Mediatech, Manassas, VA), 292 μg/ml L-Glutamine (Mediatech) and 100 μg/ml of Primocin (Invivogen, San Diego, CA). Alternatively, IPF lung explant suspensions were stained with anti-CD45-PE/Cy7, anti-CD3-PE, anti-CD28-APC and DAPI (Biolegend). $DAPI^-$ $CD45^+$ $CD3^+$ $CD28^+$ and $DAPI^-$ $CD45^+$ $CD3^+$ $CD28^-$ cells were FACS sorted using a BD Influx cell sorter (BD Biosciences). All treatments were

performed in duplicates or triplicate (depending on the T cell yield). As control, A549 cells cultured alone were utilized. T cells were then stimulated with ImmunoCult™ Human CD3/CD28 T cell activator (STEMCELL Technologies) and the cells were allowed to settle on the A549 epithelial cells for 30 minutes at room temperature. After 30 minutes, 96 well plate was placed into an IncuCyte ZOOM live cell imager (Essen Biosciences) and images were acquired under phase and red fluorescence conditions every 2–3 hours for 3–5 days. The number of red nuclei was then quantified using IncuCyte ZOOM software version 2016B (Essen Biosciences). Images were then exported and the number of nuclei over time was graphed using GraphPad prism software version 7.0d (GraphPad)

Mice:

All mouse studies were approved by IACUC and Comparative medicine at Cedars-Sinai Medical Center. Six to eight-week old Pathogen free NOD Cg-Prkdc<SCID> IL2rg<Tm1wil>Szi (NSG) were purchased from Jackson laboratories and housed in Cedars-Sinai Medical Center's high isolation animal rooms. Mice were allowed a minimum of one week to acclimate, and 1×10^6 mixed cells or $1–2 \times 10^5$ purified T cells were then injected intravenously into groups of 5 NSG mice or more. Mice were sacrificed after 35, 63 or 65 days. Dexamethasone treated mice were treated with veterinary grade dexamethasone solution (VetOne) at 10 mg/kg intraperitoneally, twice a week for five weeks. To determine the role of immune checkpoint pathways in our humanized NSG model, mixed IPF explant cell-xenografted NSG mice were treated with 5 mg/kg of anti-PD-1 (Opdivo), anti-CTLA-4 (Ipilimumab) or IgG control antibodies (IgG_4 or IgG_1, respectively) twice a week for four weeks. After a total of five weeks, mice were sacrificed, and their lungs were collected for flow cytometric, histologic and biochemical analysis. BAL fluid was collected for protein analysis, the superior and middle lobes were collected for biochemical hydroxyproline quantification, the inferior lobe for flow cytometric analysis.

Histological analysis:

Left lung tissue was fixed in 10% NBF solution for 24 hours and subsequently transferred into tissue cassettes and placed into a 70% ethanol solution for a minimum of 24 hours. Tissues where paraffin embedded, sectioned, and stained with Masson's trichrome. For Picrosirius red staining, slides were deparaffinized and hydrated, stained with hematoxylin for one minute and then for one hour in a Picrosirius red solution (5 grams Sirius red F3B (Sigma-Aldrich) in 500 ml of saturated aqueous Picric acid solution (Sigma-Aldrich)). After staining, slides where washed in two changes of 0.05% Glacial acetic acid solution, dehydrated and mounted. Stained slides where examined using a Zeiss Axio Observer Z1 microscope and the Zeiss Zen 2012 v 1.1.2.0 software (Zeiss).

Hydroxyproline assay:

Total lung hydroxyproline was analyzed as previously described[48]. To compare changes in hydroxyproline concentration, humanized lung samples were assayed together with hydrolyzed lung samples from naïve mice housed in the same facility and treated similarly[36].

Flow cytometry of Human Lung explant suspensions:

Human lung cells were added to flow cytometry wash/staining buffer and blocked with anti-human Fc receptor antibodies (Biolegend) for 15 min at 4 °C. After blocking, cells were stained with anti-human CD45, EpCAM, CD3, CD8, CD4, CD45RO, CD45RA, CD28, CTLA4, PD-1 and/or PD-L1 antibodies (Biolegend) for 20 minutes at 4 °C. Unstained, isotype and fluorescent minus one controls (Figure S8) were utilized to gate out any non-specific antibody binding and background fluorescence. Cells were then washed twice with flow cytometry wash/staining buffer, fixed in 5% neutral buffered formalin. Flow cytometric data were acquired using a MACSQuant 10 (Miltenyi Biotech) flow cytometer and data were analyzed using Flowjo software V10.2 (Treestar Inc.).

Statistical analysis:

All statistical analyses were performed using GraphPad Prism software version 7.0d (GraphPad).

Supplementary Material

Refer to Web version on PubMed Central for supplementary material.

Acknowledgments:

These studies were supported by funds and reagents from: Bristol-Myers Squibb, Boehringer, Cedars-Sinai Medical Center, and the National Institute of Health (R01HL123899). DMH was supported by Cedars-Sinai Medical Center, Boehringer and the National Institute of Health (T32-HL007517–30). The authors would like to also acknowledge Edo Israely for his help with the FACS sorting, Kathy McClinchey and McClinchey Histology Lab Inc for the histological services, the Cedars-Sinai genomics, biobank and flow cytometric cores and members of Dr. Barry Stripp's laboratory for their help in acquiring the patient and donor tissues.

Disclosure/ Conflict of Interest:

Bristol-Myers Squibb funded the studies using anti-PD-1 and anti-CTLA4 mAbs and provided the antibodies.

References:

1. du Bois RM. Strategies for treating idiopathic pulmonary fibrosis. Nature reviews Drug discovery 2010; 9(2): 129–140. [PubMed: 20094055]
2. Hecker L, Thannickal VJ. Nonresolving fibrotic disorders: idiopathic pulmonary fibrosis as a paradigm of impaired tissue regeneration. The American journal of the medical sciences 2011; 341(6): 431–434. [PubMed: 21613929]
3. Huang Y, Ma SF, Espindola MS, Vij R, Oldham JM, Huffnagle GB et al. Microbes Are Associated with Host Innate Immune Response in Idiopathic Pulmonary Fibrosis. Am J Respir Crit Care Med 2017; 196(2): 208–219. [PubMed: 28157391]
4. Zhang L, Wang Y, Pandupuspitasari NS, Wu G, Xiang X, Gong Q et al. Endoplasmic reticulum stress, a new wrestler, in the pathogenesis of idiopathic pulmonary fibrosis. Am J Transl Res 2017; 9(2): 722–735. [PubMed: 28337301]
5. Fernandez IE, Greiffo FR, Frankenberger M, Bandres J, Heinzelmann K, Neurohr C et al. Peripheral blood myeloid-derived suppressor cells reflect disease status in idiopathic pulmonary fibrosis. Eur Respir J 2016; 48(4): 1171–1183. [PubMed: 27587556]
6. Kahloon RA, Xue J, Bhargava A, Csizmadia E, Otterbein L, Kass DJ et al. Patients with idiopathic pulmonary fibrosis with antibodies to heat shock protein 70 have poor prognoses. Am J Respir Crit Care Med 2013; 187(7): 768–775. [PubMed: 23262513]

7. Hogaboam CM, Trujillo G, Martinez FJ. Aberrant innate immune sensing leads to the rapid progression of idiopathic pulmonary fibrosis. Fibrogenesis Tissue Repair 2012; 5(Suppl 1): S3. [PubMed: 23259678]
8. Gilani SR, Vuga LJ, Lindell KO, Gibson KF, Xue J, Kaminski N et al. CD28 down-regulation on circulating CD4 T-cells is associated with poor prognoses of patients with idiopathic pulmonary fibrosis. PLoS One 2010; 5(1): e8959. [PubMed: 20126467]
9. Feghali-Bostwick CA, Tsai CG, Valentine VG, Kantrow S, Stoner MW, Pilewski JM et al. Cellular and humoral autoreactivity in idiopathic pulmonary fibrosis. J Immunol 2007; 179(4): 2592–2599. [PubMed: 17675522]
10. Todd NW, Scheraga RG, Galvin JR, Iacono AT, Britt EJ, Luzina IG et al. Lymphocyte aggregates persist and accumulate in the lungs of patients with idiopathic pulmonary fibrosis. J Inflamm Res 2013; 6: 63–70. [PubMed: 23576879]
11. Lympany PA, Southcott AM, Welsh KI, Black CM, Boylston AW, du Bois RM. T-cell receptor gene usage in patients with fibrosing alveolitis and control subjects. Eur J Clin Invest 1999; 29(2): 173–181. [PubMed: 10093005]
12. Shimizudani N, Murata H, Keino H, Kojo S, Nakamura H, Morishima Y et al. Conserved CDR 3 region of T cell receptor BV gene in lymphocytes from bronchoalveolar lavage fluid of patients with idiopathic pulmonary fibrosis. Cin Exp Immunol 2002; 129(1): 140–149.
13. Idiopathic Pulmonary Fibrosis Clinical Research N, Raghu G, Anstrom KJ, King TE, Jr., Lasky JA, Martinez FJ. Prednisone, azathioprine, and N-acetylcysteine for pulmonary fibrosis. N Engl J Med 2012; 366(21): 1968–1977. [PubMed: 22607134]
14. Herazo-Maya JD, Noth I, Duncan SR, Kim S, Ma SF, Tseng GC et al. Peripheral blood mononuclear cell gene expression profiles predict poor outcome in idiopathic pulmonary fibrosis. Sci Transl Med 2013; 5(205): 205ra136.
15. Hodge G, Jersmann H, Tran HB, Holmes M, Reynolds PN, Hodge S. Lymphocyte senescence in COPD is associated with loss of glucocorticoid receptor expression by pro-inflammatory/cytotoxic lymphocytes. Respir Res 2015; 16(1): 2. [PubMed: 25573300]
16. Hodge G, Jersmann H, Tran HB, Roscioli E, Holmes M, Reynolds PN et al. Lymphocyte senescence in COPD is associated with decreased histone deacetylase 2 expressio by pro-inflammatory lymphocytes. RespirRes 2015; 16(1): 130.
17. Hodge G, Roscioli E, Jersmann H, Tran HB, Holmes M, Reynolds PN et al. Steroid resistance in COPD is associated with impaired molecular chaperone Hsp90 expression by pro-inflammatory lymphocytes. Respir Res 2016; 17(1): 135. [PubMed: 27769261]
18. Meijers RW, Litjens NH, de Wit EA, Langerak AW, van der Spek A, Baan CC et al. Cytomegalovirus contributes partly to uraemia-associated premature immunological ageing of the T cell compartment. Clin Exp lmmunol 2013; 174(3): 424–432.
19. Pieper J, Snir O, Johansson S, Janson P, Winqvist O, Malmstrom V. CD4+CD28null T cells in RA show distinctive proinflammatory features and IFN-promoter demethylation. Annals of the Rheumatic Diseases 2011; 70(Suppl 2): A46–A46.
20. Loell I, Pandya J, Raghvan S, Zong M, Malmström V, Lundberg IE. Persisting CD28nullT cells, but not regulatory T cells, in muscle tissue of myositis patients after immunosuppressive therapy. Annals of the Rheumatic Diseases 2012; 71(Suppl 1): A44.41–A44.
21. Pandya JM, Loell I, Hossain MS, Zong M, Alexanderson H, Raghavan S et al. Effects of conventional immunosuppressive treatment on CD244+ (CD28null) and FOXP3+ T cells in the inflamed muscle of patients with polymyositis and dermatomyositis. Arthritis Res Ther 2016; 18(1): 80. [PubMed: 27039301]
22. Monteiro J, Batliwalla F, Ostrer H, Gregersen PK. Shortened telomeres in clonally expanded CD28−CD8+ T cells imply a replicative history that is distinct from their CD28+CD8+ counterparts. Journal of immunology (Baltimore, Md : 1950) 1996; 156(10): 3587–3590.
23. Dvergsten JA, Mueller RG, Griffin P, Abedin S, Pishko A, Michel JJ et al. Premature cell senescence and T cell receptor-independent activation of CD8+ T cells in juvenile idiopathic arthritis. Arthritis Rheum 2013; 65(8): 2201–2210. [PubMed: 23686519]

24. Vallejo AN, Weyand CM, Goronzy JJ. T-cell senescence: a culprit of immune abnormalities in chronic inflammation and persistent infection. Trends Mol Med 2004; 10(3): 119–124. [PubMed: 15102354]
25. Vallejo AN. CD28 extinction in human T cells: altered functions and the program of T-cell senescence. Immunol Rev 2005; 205: 158–169. [PubMed: 15882352]
26. Hodge G, Hodge S, Ahern J, Holmes-Liew CL, Reynolds PN, Holmes M. Targeting Steroid Resistant Peripheral Blood Pro-Inflammatory CD28null T Cells by Inhibiting CD137 Expression: Relevance to BOS. The Journal of Heart and Lung Transplantation 2013; 32(4).
27. Slot MC, Kroon AA, Damoiseaux J, Theunissen R, Houben A, de Leeuw PW et al. CD4(+)CD28(null) T Cells are related to previous cytomegalovirus infection but not to accelerated atherosclerosis in ANCA-associated vasculitis. Rheumatol Int 2017; 37(5): 791–798. [PubMed: 28084533]
28. Tan DB, Amran FS, Teo TH, Price P, Moodley YP. Levels of CMV-reactive antibodies correlate with the induction of CD28(null) T cells and systemic inflammation in chronic obstructive pulmonary disease (COPD). Cell Mol Immunol 2016; 13(4): 551–553. [PubMed: 27402584]
29. Garcia de Tena J, Manzano L, Leal JC, San Antonio E, Sualdea V, Alvarez-Mon M. Active Crohn's disease patients show a distinctive expansion of circulating memory CD4+CD45RO +CD28null T cells. J Clin Immunol 2004; 24(2): 185–196. [PubMed: 15024186]
30. Thewissen M, Somers V, Hellings N, Fraussen J, Damoiseaux J, Stinissen P. CD4+CD28null T cells in autoimmune disease: pathogenic features and decreased susceptibility to immunoregulation. J Immunol 2007; 179(10): 6514–6523. [PubMed: 17982040]
31. Suarez-Alvarez B, Rodriguez RM, Schlangen K, Raneros AB, Marquez-Kisinousky L, Fernandez AF et al. Phenotypic characteristics of aged CD4(+) CD28(null) T lymphocytes are determined by changes in the whole-genome DNA methylation pattern. Aging Cell 2017; 16(2): 293–303. [PubMed: 28026094]
32. Hodge G, Hodge S, Ahern J, Holmes-Liew CLL, Reynolds PN, Holmes M. Up-regulation of alternate co-stimulatory molecules on proinflammatory CD28null T cells in bronchiolitis obliterans syndrome. Clinical and experimental immunology 2013; 173(1): 150–160. [PubMed: 23607447]
33. Hodge G, Hodge S. Steroid Resistant CD8(+)CD28(null) NKT-Like Pro-inflammatory Cytotoxic Cells in Chronic Obstructive Pulmonary Disease. Front Immunol 2016; 7: 617. [PubMed: 28066427]
34. Berg M, Zavazava N. Regulation of CD28 expression on CD8+ T cells by CTLA-4. J Leukoc Biol 2008; 83(4): 853–863. [PubMed: 18162511]
35. Weng NP, Akbar AN, Goronzy J. CD28(−) T cells: their role in the age-associated decline of immune function. Trends Immunol 2009; 30(7): 306–312. [PubMed: 19540809]
36. Habiel DM, Espindola MS, Coelho AL, Hogaboam CM. Modeling Idiopathic Pulmonary Fibrosis in Humanized Severe Combined Immunodeficiency Mice. Am J Pathol2018.
37. Adegunsoye A, Hrusch CL, Bonham CA, Jaffery MR, Blaine KM, Sullivan M et al. Skewed Lung CCR4 to CCR6 CD4+ T Cell Ratio in Idiopathic Pulmonary Fibrosis Is Associated with Pulmonary Function. Front Immunol 2016; 7: 516. [PubMed: 27933058]
38. Hodge G, Jersmann H, Tran HB, Holmes M, Reynolds PN, Hodge S. Lymphocyte senescence in COPD is associated with loss of glucocorticoid receptor expression by pro-inflammatory/cytotoxic lymphocytes. Respir Res 2015; 16: 2. [PubMed: 25573300]
39. Hodge G, Jersmann H, Tran HB, Roscioli E, Holmes M, Reynolds PN et al. Lymphocyte senescence in COPD is associated with decreased histone deacetylase 2 expression by pro-inflammatory lymphocytes. Respir Res 2015; 16: 130. [PubMed: 26498345]
40. Dumitriu IE. The life (and death) of CD4+ CD28(null) T cells in inflammatory diseases. Immunology 2015; 146(2): 185–193. [PubMed: 26190355]
41. Hodge G, Mukaro V, Reynolds PN, Hodge S. Role of increased CD8/CD28(null) T cells and alternative co-stimulatory molecules in chronic obstructive pulmonary disease. Clin Exp Immunol 2011; 166(1): 94–102. [PubMed: 21910726]
42. Strioga M, Pasukoniene V, Characiejus D. CD8+ CD28− and CD8+ CD57+ T cells and their role in health and disease. Immunology 2011; 134(1): 17–32. [PubMed: 21711350]

43. Sisson TH, Mendez M, Choi K, Subbotina N, Courey A, Cunningham A et al. Targeted injury of type II alveolar epithelial cells induces pulmonary fibrosis. Am J Respir Crit Care Med 2010; 181(3): 254–263. [PubMed: 19850947]

44. Glasser JR, Mallampalli RK. Surfactant and its role in the pathobiology of pulmonary infection. Microbes Infect 2012; 14(1): 17–25. [PubMed: 21945366]

45. Naidoo J, Page DB, Wolchok JD. Immune checkpoint blockade. Hematol Oncol Clin North Am 2014; 28(3): 585–600. [PubMed: 24880949]

46. Pardoll DM. The blockade of immune checkpoints in cancer immunotherapy. Nat Rev Cancer 2012; 12(4): 252–264. [PubMed: 22437870]

47. Okazaki T, Honjo T. PD-1 and PD-1 ligands: from discovery to clinical application. Int Immunol 2007; 19(7): 813–824. [PubMed: 17606980]

48. Habiel DM, Espindola MS, Coelho AL, Hogaboam CM. Modeling Idiopathic Pulmonary Fibrosis in Humanized SCID Mice. Am J Pathol 2018.

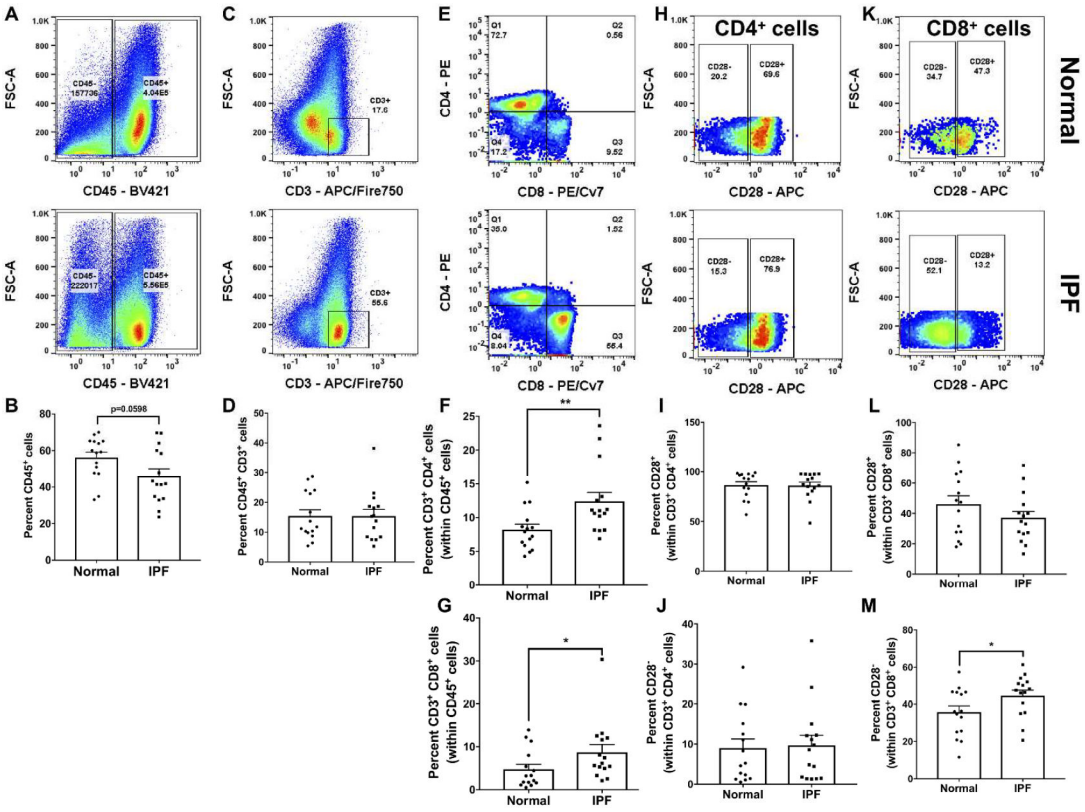

Figure 1: Abundance of CD8$^+$ CD28$^-$ T cells in IPF lung cellular suspensions.

Normal and IPF explanted lung tissues were mechanically minced to release loosely adherent and non-adherent cells. The resulting cellular suspensions was stained with anti-CD45, CD3, CD4, CD8 and CD28 antibodies. Depicted are dot plots (**A, C, E, H &K**) and average percentages (**B, D, F, G, I, J, L & M**) of CD45 (**A-B**), CD3 (**C-D**), CD4 & CD8 (**E-G**), CD28 within CD4$^+$ (**H-J**) and CD28 within CD8$^+$ (**K-M**) stained cells. Dot plots from normal and IPF samples are depicted on the top and bottom, respectively. Data shown are mean ± s.e.m; n=15/group. P values are indicated or *p ≤ 0.05 **p ≤0.01 via two-tailed Mann-Whitney non-parametric test.

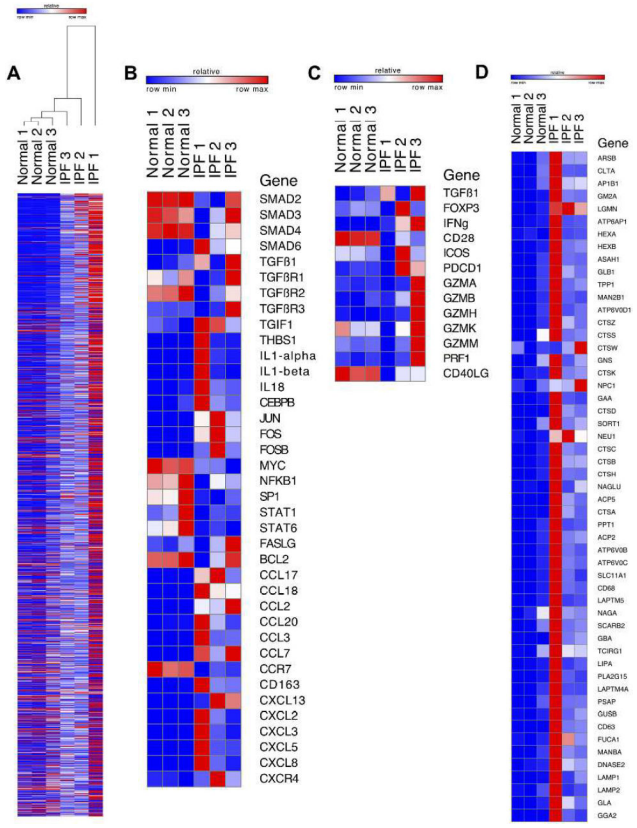

Figure 2: Enrichment of pro-inflammatory and profibrotic transcripts in IPF versus normal T cells.

Normal T cells were magnetically sorted from peripheral blood from normal donors and IPF T cells were sorted form IPF lung explant cellular suspensions, RNA was extracted and subject to RNA sequencing. Normalized FPKM values and EDGE significant transcripts were calculated using CLC workbench genomics and imported into Morpheus (Broadinstitute.org). **(A)** Depicted are significantly differentially expressed transcripts in IPF relative to normal T cells clustered using one minus Pearson correlation distance metric. **(B-D)** Depicted are heat maps generated using Morpheus of FPKM values for transcripts encoding proteins involved various pro-inflammatory and profibrotic pathways (B), T cell activation and polarization (C) and in lysosomal genesis and function (D). n=3/group.

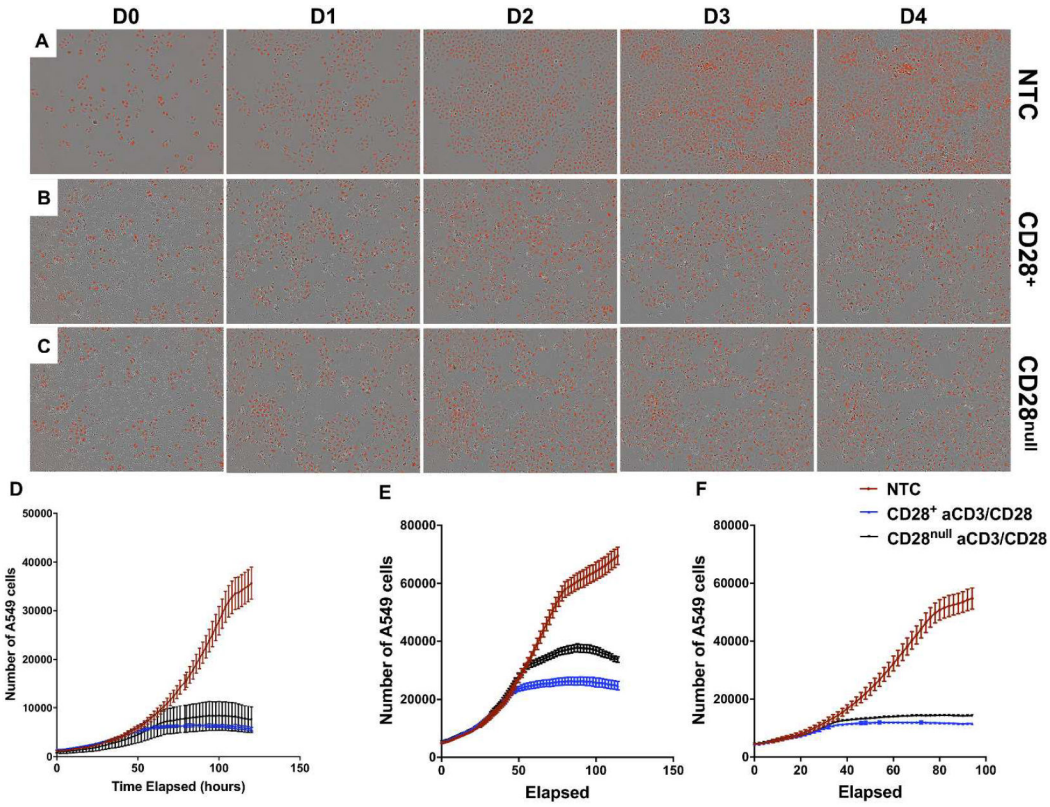

Figure 3: *In vitro* cultured CD28^{null} T cells show sim ilar anti-tumorigenic cytotoxicity to CD28^{+} T cells.

IPF lung explant cellular suspensions were stained with anti-CD28-APC antibodies. CD3^{+} CD28^{+} or CD3^{+} CD28^{null} T cells were magnetically enriched (D) or FACS sorted (E-F) from IPF lung explant cell suspensions. CD28^{+} and CD28^{-} T cells were co-cultured with NucLight Red lentivirus transduced A549 cells and the proliferation of A549 cells was monitored over-time using an Incucyte Zoom live cell imaging system. **(A-C)** Shown are representative images taken 24-hours apart of non-treated control (A), CD28^{+} T cell co-cultured (B) or CD28^{null} T cell co-cultured (C) A549 cells. **(D-F)** Shown is the number of RFP^{+} A549 cells overtime after culturing alone (red) or in the presence of IPF CD28^{+} (blue) or CD28^{null} (black) T cells. This study was performed using cells from 3 different IPF patients in triplicate.

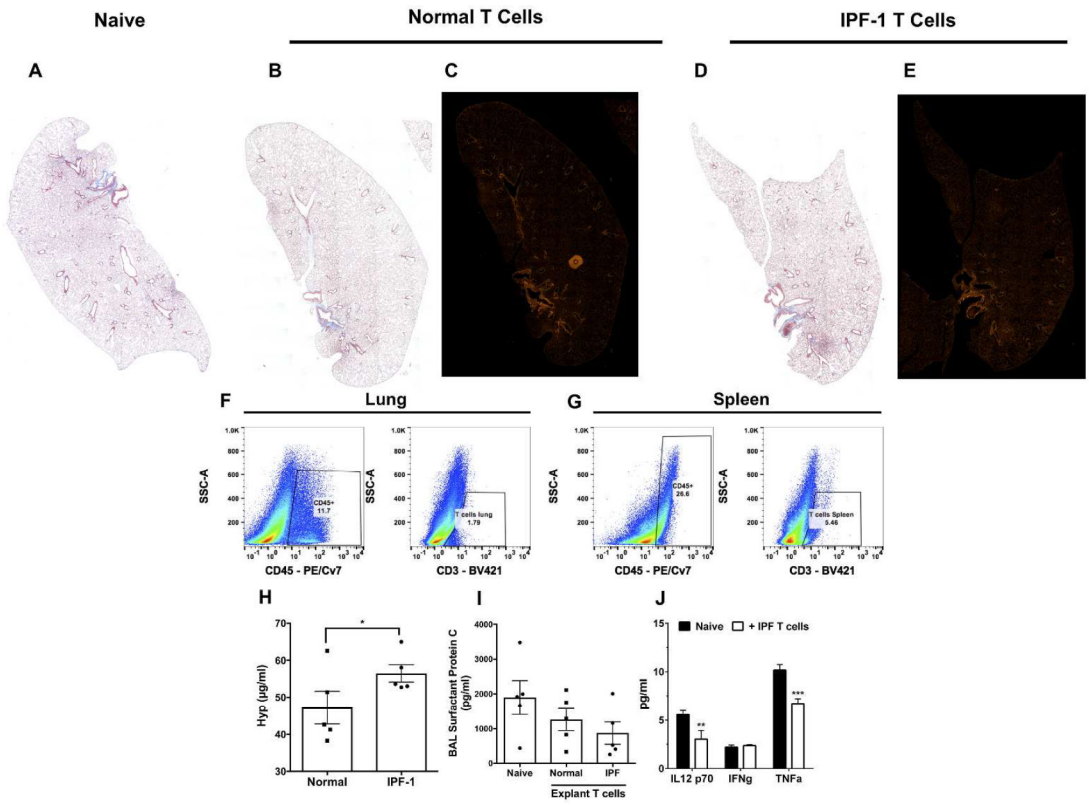

Figure 4: Lung-associated IPF T cells induced lung fibrosis in NSG mice.

Normal or IPF lung-associated T cells were FACS or magnetically sorted from lung explants. One hundred thousand cells were intravenously administered into NSG mice and 65 days after injection, mice were sacrificed, their lungs and spleens were collected for histological and flow cytometric analysis. **(A-E)** Depicted are whole mount images of Masson's Trichrome (A, B & D) or Picrosirius red (C & E) stained lungs from Naïve (A) normal (B-C) and IPF lung explant derived T cell (D-E) challenged mice. Shown are representative images from mice challenged with T cells from one normal and two IPF patients. **(F-G)** Shown are representative flow cytometric dot plots depicting human CD45 (left) and CD3 (right) expressing cells in the lungs (left) and the spleens (right) of NSG mice challenged with IPF T cells. **(H)** Shown is the average hydroxyproline concentration from the lungs of NSG mice given either normal or IPF T cells. Data shown are mean ± s.e.m; n=5 mice/group. **$p \leq 0.01$ via one-tailed Mann-Whitney non-parametric test. **(I)** One milliliter of BAL was collected from naive or T cell challenged mice. Depicted is the average surfactant protein C concentration in the BAL of naïve, normal or IPF T cell challenged NSG mice. **(J)** Depicted is the average IL12-p70, IFN-gamma (IFNγ) and TNF-alpha (TNFα) in the BAL from 3–5 naïve or IPF T-cell humanized mice per group. These studies were performed using T cells derived from one IPF patient (IPF1) and one normal donor lung. Data shown are mean ± s.e.m; n=3–5 mice/group **p = 0.0063 ***p = 0.0002 via 2way-ANOVA Sidak-corrected.

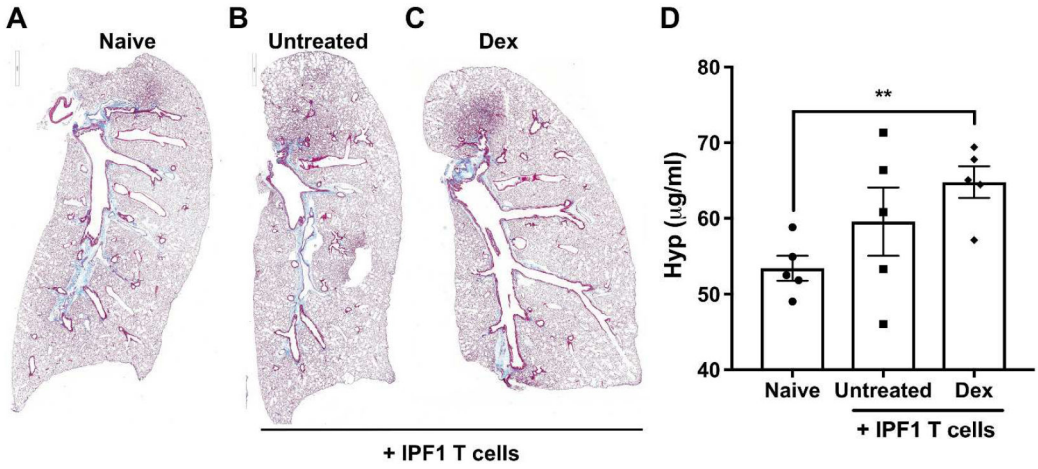

Figure 5: IPF explant T cells enriched with CD28^{null} cells are resistant to dexamethasone treatment in NSG mice.

IPF-1 lung associated T cells were intravenously administered into NSG mice. One group was treated with 10 mg/kg of Dexamethasone (Dex) intraperitoneally twice a week for 5 weeks. After a total of 5 weeks, NSG mice were sacrificed, their lungs were collected for histological and biochemical quantification of hydroxyproline concentration. (**A-C**) Depicted are whole mount images of Masson's Trichrome stained lungs from Naïve (A) IPF T cell challenged, Untreated (B) or Dex treated (C) NSG mice. (**D**) Shown is the average hydroxyproline concentration from the lungs of naïve, NSG mice given IPF1 T cells untreated or Dex treated. Data shown are mean ± s.e.m. n=5 mice/group. **p ≤ 0.01 via one-tailed Mann-Whitney non-parametric test. These studies were performed using T cells derived from one IPF patient (IPF1).

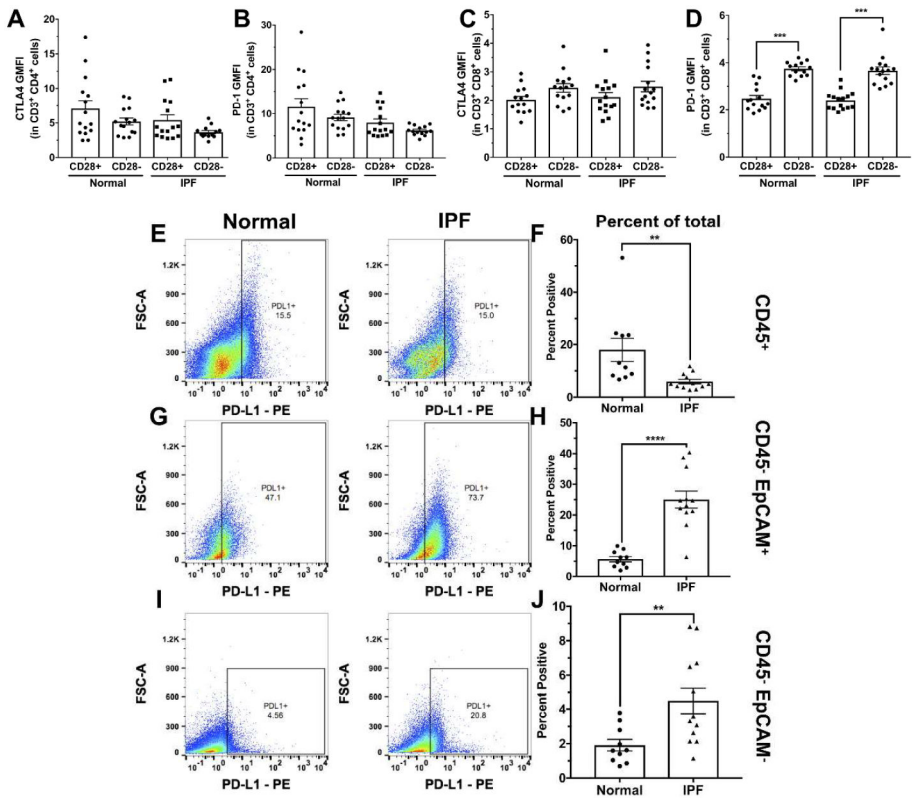

Figure 6: Abundance of PD-1 on CD8$^+$ CD28^{null} T cells and PD-LI on IPF structural cells.

Normal and IPF lung explant suspensions were stained with Anti-CD3, CD4, CD8, CD28, PD-1 and CTLA-4 antibodies. Depicted are the geometric mean fluorescence intensities (GMFI) of CTLA-4 (**A-B**) or PD-1 (**C-D**) fluorescence staining on CD3$^+$ CD4$^+$ (A & C) and CD3$^+$ CD8$^+$ (**B & D**) T cells. Data shown are mean ± s.e.m; n=14–15/group. ***p ≤ 0.001 via Kruskal-Wallis non-parametric test corrected using Dunn's multiple comparison test. (**E-J**) Flow cytometric analysis of mechanically dissociated normal and IPF lung explant cellular suspensions for cell surface PD-L1 protein. Depicted are representative dot plots of CD45$^+$ (E), CD45$^-$ EpCAM$^+$ (G) and CD45$^-$ EpCAM$^-$ (I) cells, expressing PD-L1 from normal (left) and IPF (right) lung explants. Bar graphs (F, H & J) depict the average percentage of cells expressing PD-L1 in normal or IPF lung explants. Data shown are mean ± s.e.m; n=10–12/group. **p ≤ 0.01 ****p ≤ 0.0001 via two-tailed Mann-Whitney non-parametric test.

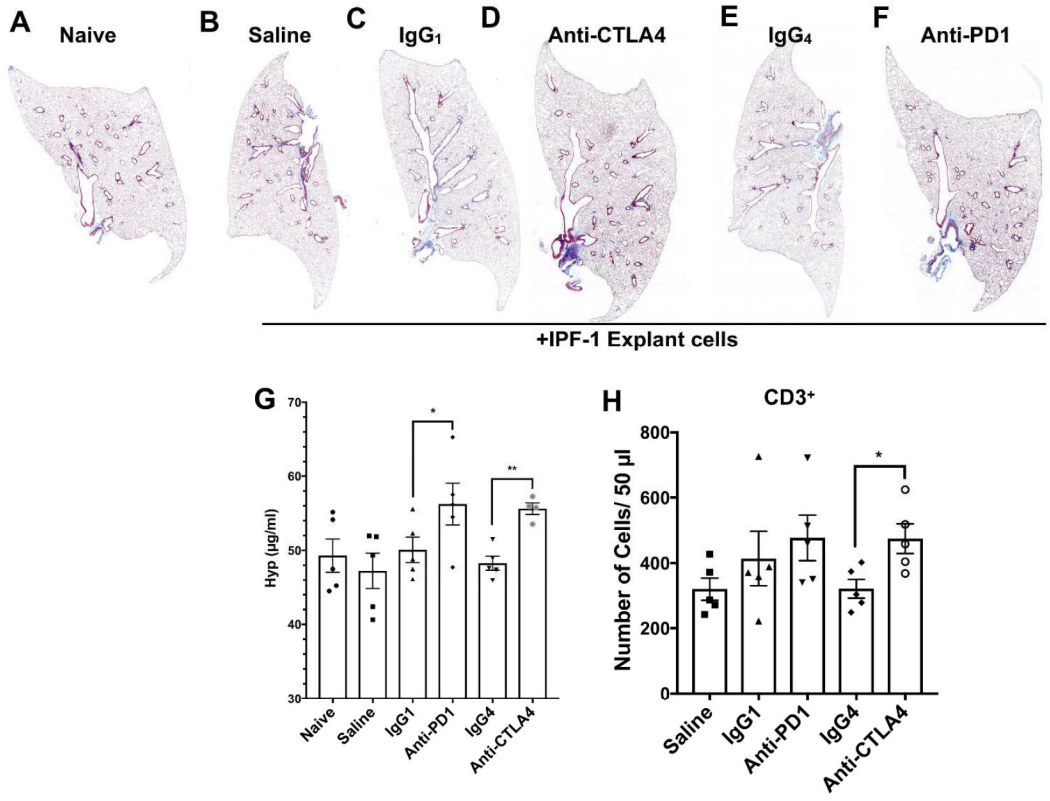

Figure 7: Targeting PD-1 or CTLA-4 in a humanized NSG model of IPF exacerbates lung remodeling.

IPF explant cells were intravenously administered into NSG mice. Seven days after administration, mice were treated with anti-PD-1, anti-CTLA4 or IgG control antibodies (5 mg/kg) twice a week for 28 days. After a total of 35 days, mice were sacrificed, their lungs were collected for flow cytometric, histological, and biochemical analysis. **(A-F)** Depicted are whole mount images of Masson's Trichrome stained lungs from Naïve (A) and IPF explant cell challenged mice, treated with saline (B), IgG_1 (C), anti-CTLA4 (D), IgG_4 (E) or anti-PD-1 (F) antibodies. **(G)** Data shown are mean ± s.e.m; n=5 mice/group. *p ≤ 0.05 **p ≤ 0.01 via one-tailed Mann-Whitney non-parametric test. **(H)** Lung cellular suspensions were generated from naïve and xenograft antibody treated NSG mice and subject to flow cytometric analysis for human CD3. Depicted is the average number of $CD3^+$ (H) cells in the lungs of NSG mice. Data shown are mean ± s.e.m; n=4–5/group. *p ≤ 0.05 via two-tailed Mann-Whitney non-parametric test. These studies were performed using T cells derived from one IPF patient (IPF1).